Stem Cell Reports Report Long Non-coding RNA T-UCstem1 Controls Progenitor Proliferation and Neurogenesis in the Postnatal Mouse Olfactory Bulb through Interaction with miR-9

Emilia Pascale, Christophe Beclin, Alessandro Fiorenzano, Gennaro Andolfi, Andrea Erni, Sandro de Falco, Gabriella Minchiotti, Harold Cremer, Annalisa Fico

▶ **To cite this version:**

Emilia Pascale, Christophe Beclin, Alessandro Fiorenzano, Gennaro Andolfi, Andrea Erni, et al.. Stem Cell Reports Report Long Non-coding RNA T-UCstem1 Controls Progenitor Proliferation and Neurogenesis in the Postnatal Mouse Olfactory Bulb through Interaction with miR-9. Current Stem Cell Reports, 2020, 15 (1-9), 10.1016/j.stemcr.2020.08.009 . hal-02951209

HAL Id: hal-02951209
https://amu.hal.science/hal-02951209

Submitted on 28 Sep 2020

HAL is a multi-disciplinary open access archive for the deposit and dissemination of scientific research documents, whether they are published or not. The documents may come from teaching and research institutions in France or abroad, or from public or private research centers.

L'archive ouverte pluridisciplinaire **HAL**, est destinée au dépôt et à la diffusion de documents scientifiques de niveau recherche, publiés ou non, émanant des établissements d'enseignement et de recherche français ou étrangers, des laboratoires publics ou privés.

Distributed under a Creative Commons Attribution 4.0 International License

Please cite this article in press as: Pascale et al., Long Non-coding RNA T-UCstem1 Controls Progenitor Proliferation and Neurogenesis in the Postnatal Mouse Olfactory Bulb through Interaction with miR-9, Stem Cell Reports (2020), https://doi.org/10.1016/j.stemcr.2020.08.009

Stem Cell Reports

Report

ISSCR

OPEN ACCESS

Long Non-coding RNA T-UCstem1 Controls Progenitor Proliferation and Neurogenesis in the Postnatal Mouse Olfactory Bulb through Interaction with miR-9

Emilia Pascale,[1,2,5] Christophe Beclin,[3,5,*] Alessandro Fiorenzano,[4] Gennaro Andolfi,[1,2] Andrea Erni,[3] Sandro De Falco,[2] Gabriella Minchiotti,[1,2] Harold Cremer,[3,6] and Annalisa Fico[1,2,6,*]

[1]Stem Cell Fate Laboratory, Institute of Genetics and Biophysics "A. Buzzati-Traverso", CNR, 80131 Naples, Italy
[2]Institute of Genetics and Biophysics "A. Buzzati-Traverso", CNR, 80131 Naples, Italy
[3]Aix-Marseille Université, CNRS, IBDM, 13288 Marseille, France
[4]Developmental and Regenerative Neurobiology, Wallenberg Neuroscience Center, and Lund Stem Cell Centre, Department of Experimental Medical Science, Lund University, 22184 Lund, Sweden
[5]Co-first author
[6]Co-senior authors
*Correspondence: christophe.beclin@univ-amu.fr (C.B.), annalisa.fico@igb.cnr.it (A.F.)
https://doi.org/10.1016/j.stemcr.2020.08.009

SUMMARY

Neural stem cell populations generate a wide spectrum of neuronal and glial cell types in a highly ordered fashion. MicroRNAs are essential regulators of this process. T-UCstem1 is a long non-coding RNA containing an ultraconserved element, and *in vitro* analyses in pluripotent stem cells provided evidence that it regulates the balance between proliferation and differentiation. Here we investigate the *in vivo* function of T-UCstem1. We show that T-UCstem1 is expressed in the forebrain neurogenic lineage that generates interneurons for the postnatal olfactory bulb. Gain of function in neural stem cells increased progenitor proliferation at the expense of neuron production, whereas knockdown had the opposite effect. This regulatory function is mediated by its interaction with miR-9-3p and miR-9-5p. Based thereon, we propose a mechanistic model for the role of T-UCstem1 in the dynamic regulation of neural progenitor proliferation during neurogenesis.

INTRODUCTION

Fine-tuning of gene expression is essential for the development and function of cells and organs. This requirement is particularly evident in the nervous system, where initially common stem cell populations generate thousands of different neuronal and glial cell types in a temporally and quantitatively perfectly orchestrated manner. MicroRNAs (miRNAs) are key components of this regulatory machinery, and over 70% of all known miRNAs are expressed in the brain (Cao et al., 2006; Landgraf et al., 2007).

Among the best-studied brain-specific miRNAs are miR-9-3p and its counterstrand miR-9-5p, which have regulatory functions in the control of neural stem cell maintenance and proliferation (Coolen et al., 2013; Follert et al., 2014). Mice with mutations in the two most abundantly expressed miR-9 loci have smaller hemispheres and olfactory bulbs (OBs) at birth, together with an enlargement of the neurogenic proliferative zones (Shibata et al., 2011).

Cellular miRNA levels and their activity are tightly controlled by transcriptional and posttranscriptional mechanisms (Wang et al., 2013; Yates et al., 2013). At the transcriptional level they are generated from discrete genomic loci, either localized in introns of coding genes, and therefore under the control of their promoters, or as independent units, positioned in intergenic regions (reviewed in Follert et al., 2014). Additional mechanisms affecting processing efficiency have been shown to regulate production of miRNA (Wang et al., 2013; Yates et al., 2013). Beyond the control of their expression, a regulatory layer relies on the sequence-dependent interaction of miRNAs with non-coding RNAs (Ebert and Sharp, 2010). Indeed, many long non-coding RNAs (lncRNAs) carry miRNA-binding sites that are able to sequester, and thereby inactivate, miRNAs (Salmena et al., 2011).

Transcribed ultraconserved elements (T-UCEs) represent an important group of lncRNAs. Whereas their full conservation among human, rat, and mouse genomes (Bejerano et al., 2004) indicates an important role (Katzman et al., 2007), their specific biological function as molecular regulators is not well understood. Notably, it has been described that a large group of ultraconserved elements in the human genome act as tissue-specific enhancers of gene expression during mouse embryonic development at 11.5 days post-conception. The majority of those enhancers direct the expression to various regions of the developing nervous system, even though their target genes are still unknown. So far, T-UCEs have been mostly studied in pathological conditions like cancer, where they can act as "natural sponges" to decoy specific miRNAs (Calin et al., 2007; Galasso et al., 2014; Olivieri et al., 2016). Evidence for roles of T-UCEs in the physiological context and during development are currently scarce (Fiorenzano et al., 2018; Panatta et al., 2020).

This is an open access article under the CC BY-NC-ND license (http://creativecommons.org/licenses/by-nc-nd/4.0/).

Please cite this article in press as: Pascale et al., Long Non-coding RNA T-UCstem1 Controls Progenitor Proliferation and Neurogenesis in the Postnatal Mouse Olfactory Bulb through Interaction with miR-9, Stem Cell Reports (2020), https://doi.org/10.1016/j.stemcr.2020.08.009

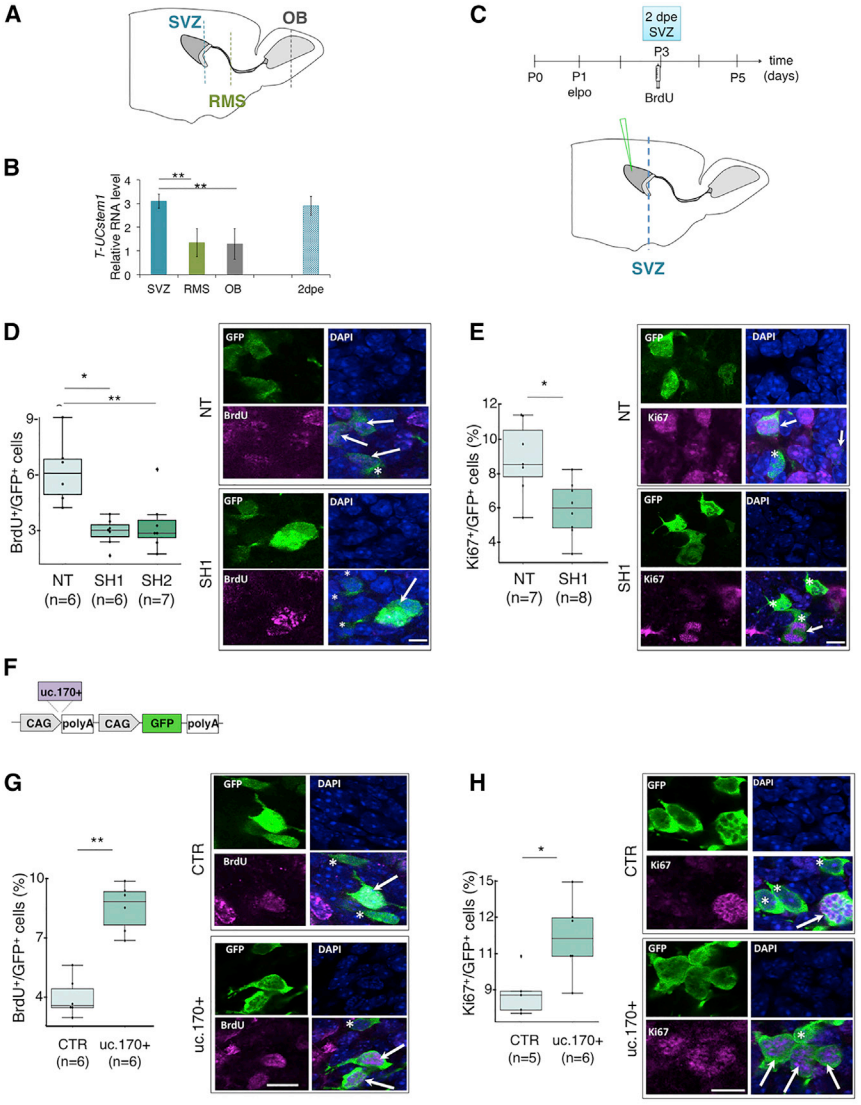

Figure 1. T-UCstem1 Controls the Proliferation of SVZ Resident Cells

(A) Schematic representation of a P1 brain.

(B) SVZ, RMS, and OB regions were dissected and used for the expression analysis. T-UCstem1 expression was analyzed by qRT-PCR. Relative RNA levels from dissected tissues and 2 days postelectroporation (dpe) sorted cells were normalized to U6 expression. Data are mean ± SEM (n = 3 independent experiments); $^{**}p < 0.005$.

(C) Timeline of the experimental plan. Electroporation (elpo) was done in mice 1 day after birth. Animals were analyzed at 2 dpe in the SVZ region, upon an intraperitoneal injection of 5-bromo-2′-deoxyuridine (BrdU; 20 mg/kg) 2 h before sacrifice.

(D) Number of $BrdU^+/GFP^+$ cells (% over the total number of GFP^+ cells) in the SVZ of control and T-UCstem1 knockdown (SH1 and SH2) animals (n = 6–7 animals; $^{*}p < 0.05$, $^{**}p < 0.005$, exact Wilcoxon test).

(E) Number of $Ki67^+/GFP^+$ cells (% over the total number of GFP^+ cells) in the SVZ of control and T-UCstem1 SH animals (n = 7–8 animals; $^{*}p < 0.05$, exact Wilcoxon test).

(F) Scheme of the bicistronic vector, driving the expression of the uc.170+ sequence and GFP reporter gene, used for T-UCstem1 gain-of-function *in vivo* experiment.

(G) Number of $BrdU^+/GFP^+$ cells (% over the total number of GFP^+ cells) in the SVZ of control (CTR) and uc.170+ overexpressing (uc.170+) mice (n = 6 animals; $^{**}p < 0.005$, exact Wilcoxon test).

(H) Number of $Ki67^+/GFP^+$ cells (% over the total number of GFP^+ cells) in the SVZ of CRT and uc.170+ animals (n = 5–6 animals; $^{*}p < 0.05$, exact Wilcoxon test).

In (D, E, G, and H) images represent high-magnification (original magnification 40×) confocal microscopy pictures showing GFP, DAPI, BrdU (D and G), or Ki67 (E and H) staining together with a merged image. White arrows: dividing cell, $GFP^+/BrdU^+$ or $Ki67^+$. White asterisks: non-dividing GFP only cell. Scale bars in (D and E), 15 μm; in (G and H), 10 μm.

We identified lncRNA T-UCstem1 as a key functional regulator of the balance between proliferation and differentiation in cultured pluripotent stem cells and showed that this activity is mediated by the therein contained uc.170 element, acting as a decoy for both miR-9-3p and miR-9-5p (Fiorenzano et al., 2018).

Here we investigate the *in vivo* function of T-UCstem1 in the brain. We show that T-UCstem1 is expressed in the postnatal forebrain neurogenic system, which generates interneurons for the OB. In this neurogenic system stem cells localized in the subventricular zone (SVZ) lining the lateral forebrain ventricles generate permanently neuronal progenitors that undergo rapid transit amplification before tangential migration via the rostral migratory stream (RMS) into the OB (Figure 1A). Here neuronal precursors detach from the RMS and integrate as local interneurons into the granule cell layer and the glomerular layer.

Using *in vivo* electroporation we demonstrate that T-UCstem1 plays a role in neurogenesis by favoring proliferation of progenitors at the expense of neuron production, thus mirroring its function during the *in vitro* differentiation of ES cells into neurons. Finally, we show that this regulatory function is mediated, at least in part, by interacting with both miR-9 strands. Based on these results we propose a

mechanistic model for a specific role of T-UCstem1 in the dynamic regulation of progenitor proliferation.

RESULTS

T-UCstem1 Is Expressed in the SVZ-RMS-OB Neurogenic System

During postnatal and adult OB neurogenesis in the mouse forebrain new neuronal precursors are permanently generated by stem cell populations along the lateral ventricles. After their rapid amplification in the SVZ they migrate via the RMS into the OB, where they integrate as local interneurons.

We investigated the presence of T-UCstem1 in this neurogenic system. qRT-PCR analyses of P1 microdissected tissue from the SVZ, RMS, and OB (Figure 1A) demonstrated that the T-UCstem1 transcript was expressed in all isolates, with significantly higher levels in the SVZ (Figure 1B).

Because dissected SVZ tissue is contaminated by non-neurogenic surrounding tissue, we investigated the expression of T-UCstem1 specifically in the neurogenic lineage. Neural stem cells were GFP labeled in 1-day-old pups (P1) by postnatal *in vivo* electroporation (Boutin et al., 2008; Bugeon et al., 2017) and GFP-positive cells were sorted by fluorescence-activated cell sorting from dissected SVZ tissue at P3 (Figure 1B). At this time point most labeled cells were fast-dividing neuronal progenitors (Boutin et al., 2008). qRT-PCR analyses demonstrated that T-UCstem1 was expressed in the GFP-labeled fraction at similar levels compared with non-sorted dissected SVZ tissue (Figure 1B). These results show that in the SVZ-RMS-OB neurogenic system T-UCstem1 is preferentially expressed in dividing progenitors of the SVZ.

T-UCstem1 Controls Proliferation of Neuronal Progenitors in the SVZ

To investigate the functional role of T-UCstem1 in OB neurogenesis, we combined loss- and gain-of-function approaches. To evaluate the effect of T-UCstem1 knockdown, we used two different non-overlapping short hairpin RNAs (shRNAs) targeting T-UCstem1 (SH1 and SH2) that lead to a significant reduction ($\geq$70%) of the transcript in mouse embryonic stem cells (ESCs). As control we used an shRNA targeting the LacZ gene (NT), as previously described (Fiorenzano et al., 2018). Control and SH1 and SH2 expression vectors were electroporated at P1 into the lateral stem cell compartment of the ventricle, together with a GFP expression construct to identify transfected cells and to monitor electroporation efficiency (Tiveron et al., 2017). Two days later, animals were injected with a single dose of bromodeoxyuridine (BrdU) and perfused 2 h later (Figure 1C). Quantification of BrdU-positive cells in the GFP-positive fraction revealed a significant loss of proliferating cells in the SVZ upon T-UCstem1 knockdown, with similar results for both SH RNAs (Figure 1D; control 6.5% ± 1.12%; SH1 3.5% ± 0.47%; SH2 3.7% ± 0.95%). Moreover, the number of Ki67-positive cells was significantly reduced after T-UCstem1 knockdown compared with control (control 9.2% ± 1.43% versus SH1 6.3% ± 1.04%) (Figure 1E). Thus, T-UCstem1 downregulation reduced proliferation of dividing progenitors in the SVZ.

Next, we evaluated the effect of the overexpression of T-UCstem1 and, in particular, of the ultraconserved region within T-UCstem1 (uc.170+) (Fiorenzano et al., 2018). A bicistronic expression plasmid driving both uc.170+ and GFP under the ubiquitous CAG promoter was generated and electroporated into the lateral ventricular wall (2×CAG-GFP-uc170+; Figure 1F and Experimental Procedures), following the Experimental Procedures described above. The electroporated mice were analyzed 2 days after electroporation. To label dividing cells, mice were injected with BrdU 2 h before sacrifice (Figure 1G). Quantitative analyses of GFP/BrdU-positive cells in the SVZ revealed that proliferating cells almost doubled in uc170+ overexpressing animals compared with control (control 4.2% ± 0.63% versus uc.170+ 8.8% ± 0.84%) (Figure 1G). In line with these findings, Ki67-positive cells significantly increased in uc170+ overexpressing animals compared with control (Figure 1H).

Thus, the combined use of loss- and gain-of-function approaches leads to the conclusion that T-UCstem1 is implicated in proliferation control of neuronal precursors in the SVZ.

T-UCstem1 Regulates Neuron Number in the OB

Next, we investigated the impact of T-UCstem1 knockdown on neuronal addition to the OB. Neural stem cells were electroporated with control and SH1-RNA vectors at P1 and the OB was analyzed 14 days later (14 dpe), when labeled cells mainly represent young neurons integrating into the OB layers (Figure 2A). Quantification revealed a significantly higher absolute number of GFP-positive neurons after T-UCstem1 knockdown (control 273 ± 3; SH1 397 ± 45; Figure 2B). Moreover, we normalized the GFP-positive neurons in the OB to the amounts of GFP-labeled cells that remained in the SVZ after electroporation and did not enter the RMS/OB (mainly radial glia, astrocytes, and ependymocytes; Boutin et al., 2008, and our unpublished data). The increased ratio further supported the conclusion that T-UCstem1 knockdown increased the production of new NeuN-positive neurons in the OB (Figures 2C and 2D).

Next, we investigated the impact of uc170+ overexpression on neuron addition to the OB. Fourteen days after

Please cite this article in press as: Pascale et al., Long Non-coding RNA T-UCstem1 Controls Progenitor Proliferation and Neurogenesis in the Postnatal Mouse Olfactory Bulb through Interaction with miR-9, Stem Cell Reports (2020), https://doi.org/10.1016/j.stemcr.2020.08.009

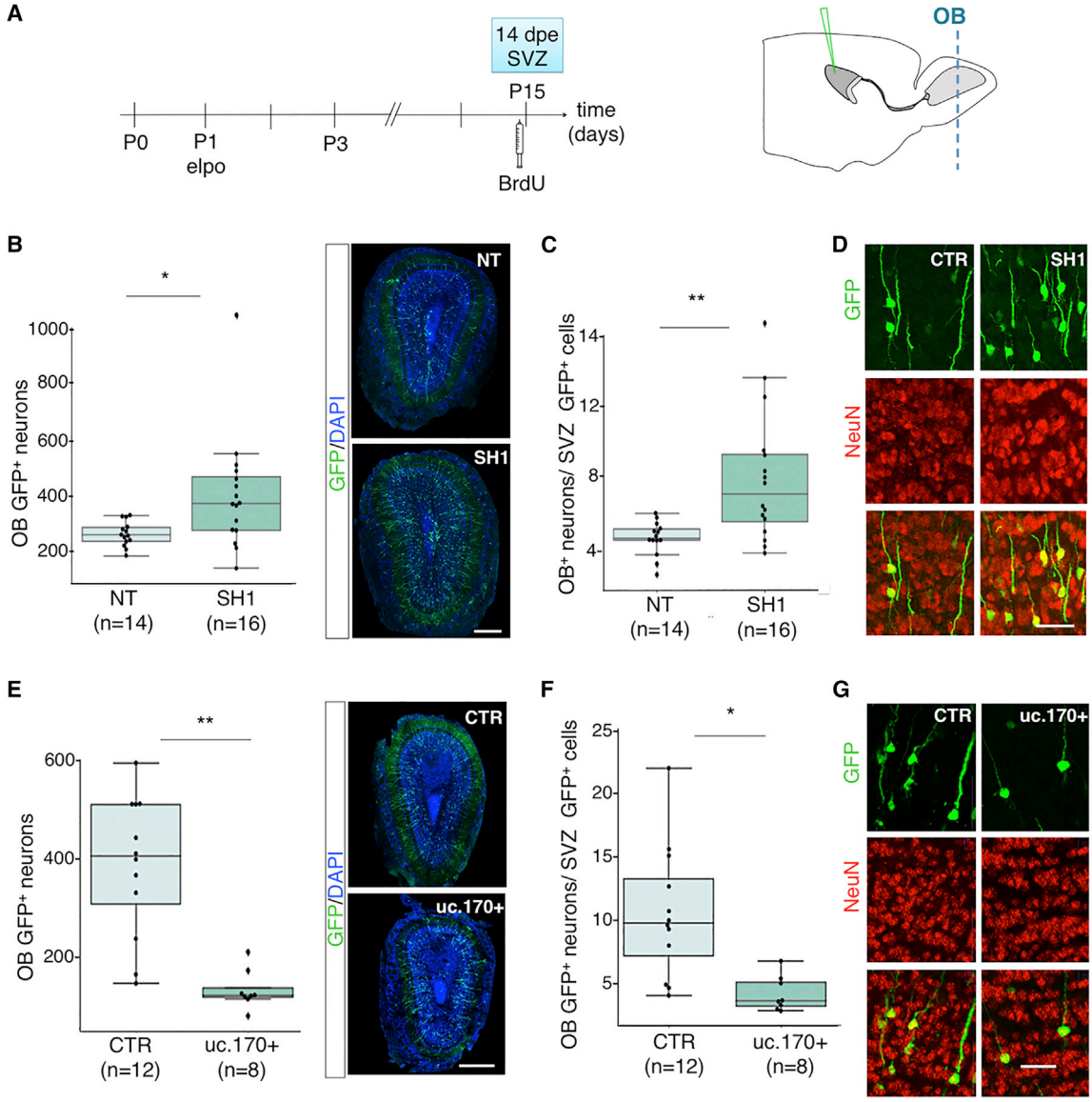

Figure 2. T-UCstem1 Contributes to Determining the Neuron Number in the Olfactory Bulb

(A) Timeline of the experimental plan. Electroporation (elpo) was done in mice 1 day after birth. Animals were analyzed 14 days post-electroporation (dpe) at the OB level.

(B) Absolute GFP$^+$ neuron numbers in the OB of NT and T-UCstem1 SH animals (n = 14–16 animals; *p < 0.05, exact Wilcoxon test). Images are representative mosaic apotome pictures of whole coronal OB sections at 14 dpe of NT and SH1 mice (original magnification 10×). Scale bar, 200 μm.

(C) GFP$^+$ neuron numbers in the OB relative to the amount of GFP$^+$ cells remaining in the SVZ after shLacZ (NT) or SH1 electroporation (n = 14–16 animals; **p < 0.005, exact Wilcoxon test).

(D) Representative pictures of NeuN immunostaining of OB coronal section in CTR and SH1 electroporated mice (original magnification 20×).

(E) Absolute GFP$^+$ neuron numbers in the OB of CTR and uc.170+ mice, at 14 dpe (n = 12–8 animals; **p < 0.005, exact Wilcoxon test). Images are representative mosaic apotome pictures of whole coronal OB sections at 14 dpe of CTR and uc.170+ mice (original magnification 10×). Scale bar, 200 μm.

(F) GFP$^+$ neuron numbers in the OB relative to the amount of GFP$^+$ cells remaining in the SVZ 14 days after CTR or uc.170+ electroporation (n = 12–8 animals; *p < 0.05, exact Wilcoxon test).

(G) Representative pictures of NeuN immunostaining of OB coronal section in CTR and uc.170+ electroporated mice (original magnification 20×). Scale bar, 40 μm. GFP$^+$ cells express NeuN.

Please cite this article in press as: Pascale et al., Long Non-coding RNA T-UCstem1 Controls Progenitor Proliferation and Neurogenesis in the Postnatal Mouse Olfactory Bulb through Interaction with miR-9, Stem Cell Reports (2020), https://doi.org/10.1016/j.stemcr.2020.08.009

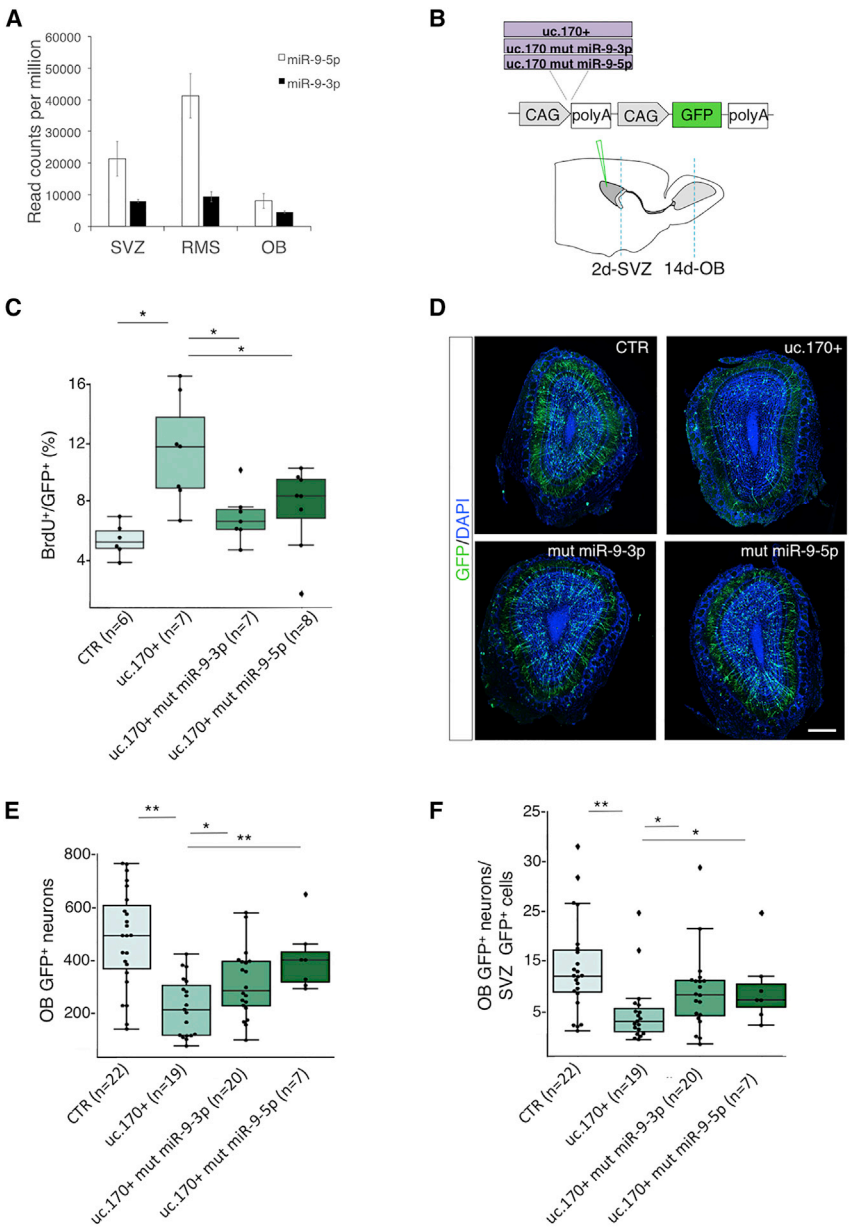

Figure 3. Functional Interaction between T-UCstem1 and miR-9 in the SVZ-RMS-OB Neurogenic System

(A) Deep-sequencing analyses of miR-9-3p and miR-9-5p expression in microdissected tissue from the SVZ, RMS, and OB.

(B) Scheme of the bicistronic vector carrying the uc.170+ sequence mutated in the seed sequences for miR-9-3p and miR-9-5p, together with the GFP reporter gene. CTR, uc170+, and both mutated miR-9 (uc.170+ mut miR-9-3p and miR-9-5p) vectors were individually electroporated into the postnatal SVZ of 1-day-old pups (P1). Animals were analyzed 2 dpe at the SVZ level, upon an intraperitoneal injection of BrdU 2 h before sacrifice, or at 14 dpe at the OB level.

(C) The chart shows the percentage of GFP^+/$BrdU^+$ cells (% over the total number of GFP^+ cells) defined in the four experimental conditions (n = 6–8 animals; *p < 0.05, exact Wilcoxon test).

(D) Representative mosaic images of coronal OB sections at 14 dpe (apotome images; original magnification 10×). Scale bar, 200 μm. Electroporation of CTR, uc170+, and both mutated miR-9 vectors was done in 1-day-old pups (P1), and effects were analyzed.

(E) Absolute GFP^+ neuron numbers in the OB of the four conditions in mice at 14 dpe (n = 7–22 animals; *p < 0.05, **p < 0.005, exact Wilcoxon test).

(F) GFP^+ neuron numbers in the OB relative to the amount of GFP^+ cells remaining in the SVZ after electroporation (n = 7–22 animals; *p < 0.05, **p < 0.005, exact Wilcoxon test).

electroporation of the 2×CAG-GFP-uc170+ plasmid, the absolute number of GFP-positive neurons in the OB was reduced by more than 50% in uc170+ overexpressing mice (Figure 2E). This reduction in new neurons was also obvious after normalization to the number of cells that remained in the SVZ, as above, arguing against large differences in electroporation efficiency (Figure 2F). Remaining neurons were correctly localized, showed normal morphology, and expressed NeuN (Figure 2G).

Altogether these findings show that the level of T-UCstem1 expression contributes to balancing progenitor proliferation and neuron production.

T-UCstem1 Interacts with miR-9-3p and miR-9-5p

The uc.170 element carries the seed sequences for both mature forms of miR-9, miR-9-3p and miR-9-5p, and acts as a decoy for these miRNAs, thereby inhibiting their action and keeping mouse ESCs in a proliferative state (Fiorenzano et al., 2018). Deep sequencing of microdissected tissue from the SVZ, RMS, and OB demonstrated that both miR-9 strands were expressed in all three isolates (Figure 3A) (Beclin et al., 2016). Expression was strong in the SVZ, peaked in the RMS, and was lowest in the OB.

To investigate the uc170::miR-9 molecular interaction during postnatal neurogenesis, we mutated either the

miR-9-5p or the miR-9-3p binding site of the uc.170 expression plasmid, as previously described (Fiorenzano et al., 2018). Wild-type uc.170, uc.170 with mutations in miR-9-3p or miR-9-5p, and empty control DNA plasmids were individually electroporated into the postnatal SVZ. The respective effects of each of these plasmids on cell proliferation at 2 dpe and neuron production at 14 dpe were analyzed and compared (Figure 3B).

At 2 dpe, wild-type uc.170+ overexpression increased cell proliferation in the GFP-positive fraction in the SVZ compared with control (control 5.8% ± 0.7% versus uc.170+ 11.8% ± 2.3%; 2-h BrdU pulse) (Figures 3C and 3D). Mutations in both the miR-9-3p and the miR-9-5p binding site of uc.170+ led to a significant rescue in the ratios of BrdU/GFP-positive cells (uc.170+ mut miR-9-3p 7.3% ± 1.1%; uc.170+ mut miR-9-5p 7.9% ± 1.9%) (Figure 3C).

At 14 dpe, we investigated the absolute number of GFP-positive neurons in the OB and their relative abundance compared with cells that remained in the SVZ. Both parameters showed significantly higher values when the miR-9-3p or miR-9-5p mutation-carrying uc.170+ vector was electroporated (Figures 3E and 3F).

Altogether these results provide evidence that T-UCstem1 regulates neural precursor proliferation and neuron number in postnatal neurogenesis in a miR-9-dependent manner.

DISCUSSION

We provide strong evidence for a function of T-UCstem1 in the control of progenitor proliferation and neuron production in the postnatal mouse forebrain via a mechanism implicating miR-9-3p and miR-9-5p. Indeed, our complementary *in vivo* gain- and loss-of-function studies are fully coherent with our previous work in ESCs (Fiorenzano et al., 2018) and represent, to our knowledge, the first demonstration of a physiological role for ultraconserved element-containing lncRNAs in the brain. The high conservation of both T-UCstem1 and miR-9 points to an important and essential interaction, which is likely to be involved in many different contexts in which stem cell proliferation has to be balanced with differentiation.

This need for balancing is well exemplified in the brain, where maintenance of stem cell pools is essential to safeguard growth and regeneration capacity at postnatal and adult stages. Indeed, during embryonic forebrain neurogenesis neural stem cells are set aside and do not participate in the massive proliferation and differentiation that leads to the development of structures like the cortex, the basal ganglia, or the septum (Fuentealba et al., 2015). After birth these quiet stem cells are sequentially activated to supply the OB with new interneurons throughout adulthood. This means that the neurogenic activity of the remaining stem cell population needs to be tightly regulated. Indeed, activation of neural stem cells by loss of Notch2 leads to increased proliferation and new neurons in the OB lineage. However, this overactivation leads in the long run to accelerated exhaustion of the stem cell pool and an aging-like phenotype (Engler et al., 2018).

After stem cell activation, the next step in the sequence that leads to new neurons is the passage to fast-dividing intermediate progenitors (or type C cells), which determines the number of new neurons produced for the OB. It is obvious that this stage needs to be again tightly controlled to adjust the generation rate of a given neuronal type. We demonstrate that the number of dividing cells in the SVZ is significantly reduced upon T-UCstem1 knockdown, whereas it increases upon T-UCstem1 overexpression. Two scenarios for T-UCstem1 function could explain this observation. First, T-UCstem1 controls activation of quiescent stem cells. In its absence more cells are activated and enter their normal proliferation program. Second, stem cell activation is independent of T-UCstem1, but the exit from the proliferative state is delayed. The observation that the production of new neurons 14 days after T-UCstem1 knockdown is inversely correlated with proliferation rate clearly supports the second hypothesis, showing that the action of T-UCstem1 is to balance between proliferative progenitors and postmitotic neuronal precursors.

Mechanistically, we propose that T-UCstem1 controls neural progenitor proliferation, at least in part, through the direct inhibitory interaction of the ultraconserved element uc170+ with the functional mature forms of miR-9. miR-9-3p and miR-9-5p are currently probably the best-characterized brain-specific miRNAs, and their implication in the control of neural stem cell status and proliferation, via the notch pathway (Roese-Koerner et al., 2016), the REST/CoREST system (Packer et al., 2008), or TLX (Zhao et al., 2009), has been intensely studied (Follert et al., 2014; Shibata et al., 2011).

Previous work demonstrated that in the adult brain about 16 cells/clone are produced from one activated stem cell in about four rounds of division (Ponti et al., 2013). It is tempting to speculate that the regulation of miR-9 activity by T-UCstem1::miR-9 interactions constitutes part of this molecular "counting mechanism," allowing the stability and flexibility to maintain the neurogenic process in the long run. How could this work?

Indeed, the choice of progenitors between proliferation and cell-cycle exit might depend on the stoichiometry between the miR-9-3p/-5p and the T-UCstem1 molecules, which is determined by their relative stability over time. miR-9-3p and miR-9-5p appear to be particularly stable miRNAs that are present in the cell for prolonged periods

(Bonev et al., 2012; Goodfellow et al., 2014). On the other hand, there is evidence that lncRNAs that contain miRNA binding sites are relatively unstable (Blumberg et al., 2020), which leads us to speculate that T-UCstem1 has a short half-life. Thus, we could consider a scenario in which initially miR-9-3p/-5p and T-UCstem1 are co-expressed in activated neural stem cells, leading to sequestering of the miRNAs and allowing clonal expansion. However, over time the rapid decay of the lncRNA would lead to the release of the stable miR-9s and allow their function as inducers of postmitotic state and differentiation.

Moreover, we cannot rule out the existence of a multilayer network controlling neurogenesis in an even more complex and subtle manner than that shown so far. Indeed, the genomic locus uc.170 shows an enriched forebrain enhancer activity (Pennacchio et al., 2006), which could be thought to be involved in some extent.

EXPERIMENTAL PROCEDURES

Tissue Dissection, Cell Dissociation, and Cell Sorting

Animals were decapitated and brains were cut into 400-μm-thick sections using a vibrating-blade microtome (Thermo Scientific, HM 650V). SVZ, RMS, and OB tissues were microdissected under a binocular microscope and kept in cold Hank's balanced salt solution (HBSS; Gibco, 14170120).

For cell sorting, dissected tissues were subjected to cell dissociation using a papain solution and mechanical dissociation as described previously (Lugert et al., 2010). Cells were resuspended in HBSS/Mg/Ca supplemented with 10 mM HEPES (Gibco, 15630080), 40 μg/mL DNase I (Roche, 10104159001), 4.5 g/L glucose (Gibco, A2494001), and 2 mM EDTA; filtered through a 30-μm preseparation filter (Miltenyi Biotec, 130-041-407); and sorted on a MoFlo Astrios EQ cytometer (Beckman-Coulter) gating on the GFP^+ population.

Quantitative RT-PCR

The relative amount of specific transcripts was measured by qRT-PCR analysis. Briefly, it was performed using a SYBR Green Supermix (Bio-Rad) protocol with a CFX96 Deep Well system real-time PCR detection system (Bio-Rad), according to the manufacturer's instructions. Small nuclear RNA U6 was used as a reference. The sequences of primers are reported in the Supplemental Experimental Procedures.

Plasmids and Postnatal Brain Electroporation

shRNA plasmids were described in Fiorenzano et al. (2018). They were electroporated into mouse brains together with a pCX-GFP plasmid (Morin et al., 2007) to label the cells. For overexpression experiments uc.170+, uc.170+ mut miR-9-3p, and uc.170+ mut miR-9-5p sequences were subcloned into the 2×CAGS-GFP plasmid. The cloning details are reported in the Supplemental Experimental Procedures. The electroporation procedure was as described in Boutin et al. (2008) and the Supplemental Experimental Procedures.

BrdU Injections and Immunofluorescence

Two days after electroporation BrdU (5-bromo-2′-deoxyuridine; Sigma) was injected intraperitoneally at 20 mg/kg body weight, and animals were sacrificed 2 h after BrdU injection and stained with an anti-BrdU antibody. The immunohistochemistry procedure is reported in the Supplemental Experimental Procedures.

Cell Counts and Statistical Analysis

All quantifications were performed blind to experimental group using ImageJ software. $BrdU^+$ or $Ki67^+$ cells among GFP^+ cells were counted in the SVZ at 2 dpe from at least three sections for each animal. The number of GFP neurons per OB section was quantified at 14 dpe from at least three sections per animal. Statistical analysis between two experimental conditions was performed using the non-parametric exact Wilcoxon test.

SUPPLEMENTAL INFORMATION

Supplemental Information can be found online at https://doi.org/10.1016/j.stemcr.2020.08.009.

AUTHOR CONTRIBUTIONS

A. Fico conceived the original idea. H.C. and A. Fico designed and supervised the study. E.P. performed experiments and analyzed the data. C.B. designed and performed experiments. A.E., A. Fiorenzano, and G.A. performed experiments. G.M. gave conceptual advice and revised the manuscript. S.D.F. provided key reagents and revised the manuscript. C.B., H.C., and A. Fico wrote the manuscript.

ACKNOWLEDGMENTS

We thank Eduardo Jorge Patriarca for his helpful contributions from the initial stage of the project and Drs. M.C. Tiveron and N. Core for support and discussions. We thank the PiCSL-FBI core facility (IBDM, AMU-Marseille) supported by the French National Research Agency through the Investments for the Future program (France-BioImaging, ANR-10-INBS-04), as well as the IBDM animal facility. We are grateful to the AMUTICYT Cytometry and Cell Sorting Core facility, AMU, UMR-S 1076. This work was supported by TRANSCAN-2 Project BeFIT, Epigenomics Flagship Project (EPIGEN) MIUR-CNR, Italian Ministry of Education University Research (grant CTN01_00177 Cluster ALISEI_IRMI) to A.F.; by project SATIN-POR Campania FESR 2014/2020 to G.M.; and by the Agence National pour la Recherche (grants ANR- 13-BSV4-0013 and ANR- 17-CE16-0025), Fondation pour la Recherche Médicale (FRM) Label Equipe FRM, and Fondation de France grant FDF70959 to H.C. A.E. was supported by a postdoctoral fellowship from the Swiss National Funds.

Received: May 17, 2020
Revised: August 22, 2020
Accepted: August 24, 2020
Published: September 24, 2020

REFERENCES

Beclin, C., Follert, P., Stappers, E., Barral, S., Coré, N., de Chevigny, A., Magnone, V., Lebrigand, K., Bissels, U., Huylebroeck, D., et al. (2016). miR-200 family controls late steps of postnatal forebrain neurogenesis via Zeb2 inhibition. Sci. Rep. *6*, 35729.

Bejerano, G., Pheasant, M., Makunin, I., Stephen, S., Kent, W.J., Mattick, J.S., and Haussler, D. (2004). Ultraconserved elements in the human genome. Science *304*, 1321–1325.

Blumberg, A., Zhao, Y., Huang, Y., Dukler, N., Rice, E.J., Chivu, A.G., Krumholz, K., Danko, C.G., and Siepel, A. (2020). Characterizing RNA stability genome-wide through combined analysis of PRO-seq and RNA-seq data. bioRxiv https://doi.org/10.1101/690644.

Bonev, B., Stanley, P., and Papalopulu, N. (2012). MicroRNA-9 Modulates Hes1 ultradian oscillations by forming a double-negative feedback loop. Cell Rep. *2*, 10–18.

Boutin, C., Diestel, S., Desoeuvre, A., Tiveron, M.C., and Cremer, H. (2008). Efficient in vivo electroporation of the postnatal rodent forebrain. PLoS One *3*, e1883.

Bugeon, S., de Chevigny, A., Boutin, C., Core, N., Wild, S., Bosio, A., Cremer, H., and Beclin, C. (2017). Direct and efficient transfection of mouse neural stem cells and mature neurons by in vivo mRNA electroporation. Development *144*, 3968–3977.

Calin, G.A., Liu, C.G., Ferracin, M., Hyslop, T., Spizzo, R., Sevignani, C., Fabbri, M., Cimmino, A., Lee, E.J., Wojcik, S.E., et al. (2007). Ultraconserved regions encoding ncRNAs are altered in human leukemias and carcinomas. Cancer Cell *12*, 215–229.

Cao, X., Yeo, G., Muotri, A.R., Kuwabara, T., and Gage, F.H. (2006). Noncoding RNAs in the mammalian central nervous system. Annu. Rev. Neurosci. *29*, 77–103.

Coolen, M., Katz, S., and Bally-Cuif, L. (2013). miR-9: a versatile regulator of neurogenesis. Front. Cell Neurosci. *7*, 220.

Ebert, M.S., and Sharp, P.A. (2010). Emerging roles for natural microRNA sponges. Curr. Biol. *20*, R858–R861.

Engler, A., Rolando, C., Giachino, C., Saotome, I., Erni, A., Brien, C., Zhang, R., Zimber-Strobl, U., Radtke, F., Artavanis-Tsakonas, S., et al. (2018). Notch2 signaling maintains NSC quiescence in the murine ventricular-subventricular zone. Cell Rep. *22*, 992–1002.

Fiorenzano, A., Pascale, E., Gagliardi, M., Terreri, S., Papa, M., Andolfi, G., Galasso, M., Tagliazucchi, G.M., Taccioli, C., Patriarca, E.J., et al. (2018). An ultraconserved element containing lncRNA preserves transcriptional dynamics and maintains ESC self-renewal. Stem Cell Reports *10*, 1102–1114.

Follert, P., Cremer, H., and Beclin, C. (2014). MicroRNAs in brain development and function: a matter of flexibility and stability. Front. Mol. Neurosci. *7*, 5.

Fuentealba, L.C., Rompani, S.B., Parraguez, J.I., Obernier, K., Romero, R., Cepko, C.L., and Alvarez-Buylla, A. (2015). Embryonic origin of postnatal neural stem cells. Cell *161*, 1644–1655.

Galasso, M., Dama, P., Previati, M., Sandhu, S., Palatini, J., Coppola, V., Warner, S., Sana, M.E., Zanella, R., Abujarour, R., et al. (2014). A large scale expression study associates uc.283-plus lncRNA with pluripotent stem cells and human glioma. Genome Med. *6*, 76.

Goodfellow, M., Phillips, N.E., Manning, C., Galla, T., and Papalopulu, N. (2014). microRNA input into a neural ultradian oscillator controls emergence and timing of alternative cell states. Nat. Commun. *5*, 3399.

Katzman, S., Kern, A.D., Bejerano, G., Fewell, G., Fulton, L., Wilson, R.K., Salama, S.R., and Haussler, D. (2007). Human genome ultraconserved elements are ultraselected. Science *317*, 915.

Landgraf, P., Rusu, M., Sheridan, R., Sewer, A., Iovino, N., Aravin, A., Pfeffer, S., Rice, A., Kamphorst, A.O., Landthaler, M., et al. (2007). A mammalian microRNA expression atlas based on small RNA library sequencing. Cell *129*, 1401–1414.

Lugert, S., Basak, O., Knuckles, P., Haussler, U., Fabel, K., Gotz, M., Haas, C.A., Kempermann, G., Taylor, V., and Giachino, C. (2010). Quiescent and active hippocampal neural stem cells with distinct morphologies respond selectively to physiological and pathological stimuli and aging. Cell Stem Cell *6*, 445–456.

Morin, X., Jaouen, F., and Durbec, P. (2007). Control of planar divisions by the G-protein regulator LGN maintains progenitors in the chick neuroepithelium. Nat. Neurosci. *10*, 1440–1448.

Olivieri, M., Ferro, M., Terreri, S., Durso, M., Romanelli, A., Avitabile, C., De Cobelli, O., Messere, A., Bruzzese, D., Vannini, I., et al. (2016). Long non-coding RNA containing ultraconserved genomic region 8 promotes bladder cancer tumorigenesis. Oncotarget *7*, 20636–20654.

Packer, A.N., Xing, Y., Harper, S.Q., Jones, L., and Davidson, B.L. (2008). The bifunctional microRNA miR-9/miR-9* regulates REST and CoREST and is downregulated in Huntington's disease. J. Neurosci. *28*, 14341–14346.

Panatta, E., Lena, A.M., Mancini, M., Smirnov, A., Marini, A., Delli Ponti, R., Botta-Orfila, T., Tartaglia, G.G., Mauriello, A., Zhang, X., et al. (2020). Long non-coding RNA uc.291 controls epithelial differentiation by interfering with the ACTL6A/BAF complex. EMBO Rep. *21*, e46734.

Pennacchio, L.A., Ahituv, N., Moses, A.M., Prabhakar, S., Nobrega, M.A., Shoukry, M., Minovitsky, S., Dubchak, I., Holt, A., Lewis, K.D., et al. (2006). In vivo enhancer analysis of human conserved non-coding sequences. Nature *444*, 499–502.

Ponti, G., Obernier, K., Guinto, C., Jose, L., Bonfanti, L., and Alvarez-Buylla, A. (2013). Cell cycle and lineage progression of neural progenitors in the ventricular-subventricular zones of adult mice. Proc. Natl. Acad. Sci. U S A *110*, E1045–E1054.

Roese-Koerner, B., Stappert, L., Berger, T., Braun, N.C., Veltel, M., Jungverdorben, J., Evert, B.O., Peitz, M., Borghese, L., and Brustle, O. (2016). Reciprocal regulation between bifunctional miR-9/9(*) and its transcriptional modulator notch in human neural stem cell self-renewal and differentiation. Stem Cell Reports *7*, 207–219.

Salmena, L., Poliseno, L., Tay, Y., Kats, L., and Pandolfi, P.P. (2011). A ceRNA hypothesis: the Rosetta Stone of a hidden RNA language? Cell *146*, 353–358.

Shibata, M., Nakao, H., Kiyonari, H., Abe, T., and Aizawa, S. (2011). MicroRNA-9 regulates neurogenesis in mouse telencephalon by targeting multiple transcription factors. J. Neurosci. *31*, 3407–3422.

Please cite this article in press as: Pascale et al., Long Non-coding RNA T-UCstem1 Controls Progenitor Proliferation and Neurogenesis in the Postnatal Mouse Olfactory Bulb through Interaction with miR-9, Stem Cell Reports (2020), https://doi.org/10.1016/j.stemcr.2020.08.009

Tiveron, M.C., Beclin, C., Murgan, S., Wild, S., Angelova, A., Marc, J., Core, N., de Chevigny, A., Herrera, E., Bosio, A., et al. (2017). Zic-proteins are repressors of dopaminergic forebrain fate in mice and C. elegans. J. Neurosci. *37*, 10611–10623.

Wang, Z., Yao, H., Lin, S., Zhu, X., Shen, Z., Lu, G., Poon, W.S., Xie, D., Lin, M.C., and Kung, H.F. (2013). Transcriptional and epigenetic regulation of human microRNAs. Cancer Lett. *331*, 1–10.

Yates, L.A., Norbury, C.J., and Gilbert, R.J. (2013). The long and short of microRNA. Cell *153*, 516–519.

Zhao, C., Sun, G., Li, S., and Shi, Y. (2009). A feedback regulatory loop involving microRNA-9 and nuclear receptor TLX in neural stem cell fate determination. Nat. Struct. Mol. Biol. *16*, 365–371.